A Ku-Band Dual Linear-Polarized 2×4 Microstrip Patch Subarray with a Rhombic Feed Transmission Line for Enhanced Cross-Polarization Cancellation

Riyani Jana Yanti
Department of Electrical Engineering, Universitas Indonesia, Depok, Indonesia | Research Center for Telecommunication, National Research and Innovation Agency, Bandung, Indonesia
riyani.jana@ui.ac.id

Aditya Inzani Wahdiyat
Research Center for Electronics, National Research and Innovation Agency, Tangerang Selatan, Indonesia
adit009@brin.go.id

Muzammil Jusoh
Advanced Computing (AdvComp) Centre of Excellence, Faculty of Electronic Engineering Technology, Universiti Malaysia Perlis, Perlis, Malaysia
muzammil@unimap.edu.my

Catur Apriono
Department of Electrical Engineering, Universitas Indonesia, Depok, Indonesia
catur@eng.ui.ac.id (corresponding author)

Received: 1 October 2025 | Revised: 14 November 2025 | Accepted: 24 November 2025

 DOI: https://doi.org/10.48084/etasr.15248

ABSTRACT

A Ku-band, dual-linear polarized, 2×4 microstrip circular patch subarray antenna with co-aligned elements and a rhombic feed transmission line to is proposed to improve cross-polarization performance, enhance link reliability, and provide a compact, single-port solution for mobile satellite terminals. This design directly addresses key limitations of existing mobile satellite antennas, including polarization mismatch and degraded performance under dynamic operating conditions. Mobile satellite systems on moving platforms, such as vehicles and emergency terminals, have difficulty maintaining polarization isolation and stable performance due to motion and varying environmental conditions. The proposed antenna is optimized for communication satellite systems, integrating with Satellite Nusantara Satu. The simulation results demonstrate good impedance matching, with an S11 of –47.43 dB at 12.55 GHz, a 659 MHz bandwidth, and a 9.28 dBi gain. However, the measured results indicate a slight frequency shift to 12.32 GHz, with an S11 of –20.51 dB, a bandwidth of 364 MHz, and a gain of 8.77 dBi, due to variations in fabrication tolerance and substrate permittivity. The subarray achieves a high Cross-Polarization Level (CPL) of more than –45 dB, confirming that the antenna is reliable for Ku-band satellite communication and provides enhanced polarization purity under continuous motion and varying environmental conditions, including vibration, temperature fluctuations, humidity, and physical obstructions.

Keywords-antenna; dual-polarized; rhombic feed; satellite; subarray

I. INTRODUCTION

Located in the Ring of Fire, Indonesia is a region highly susceptible to natural disasters, like earthquakes, tsunamis, floods, and landslides. Thus, it depends on satellite communications used as an early warning system [1]. The Satellite Nusantara Satu is a Geostationary (GEO) satellite [2], offering low latency, high-speed connectivity, and near-global coverage, while minimizing the need for a large terrestrial infrastructure [3]. The Nusantara Satu satellite features a Ku-

band transponder that provides broadband and Mobile Satellite Communications (MSC) to rural areas in Indonesia [4]. However, its frequencies above 10 GHz are susceptible to interference from heavy rain, which can degrade link quality and availability. Satellite communication offers numerous benefits, including substantial transmission capacity, wide bandwidth, global service coverage, and reliable connectivity [5]. Phased array antennas are widely used in communication satellites to improve transmission quality [6], with antenna polarization being equally important for reliable signal reception. However, factors such as multipath propagation, shadowing, and depolarizing media (e.g., rain, ice, and the ionosphere) can distort polarization [7]. Dual circularly polarized antennas help minimize multipath fading and polarization mismatch [8, 9]; yet, they pose challenges for GEO mobile platforms due to structural complexity, large dimensions, and difficulty maintaining high isolation under dynamic conditions. Most Ku-band antennas use linear polarization [10], increasing the channel capacity and spectral efficiency required by mobile platforms such as vehicles, ships, and emergency terminals [11]. This is achieved through simultaneous orthogonal transmission, improved bandwidth, and reduced interference. The development of compact, dual-polarized microstrip antennas with high isolation and stable performance remains challenging, particularly in tropical regions. Previous methods—such as aperture coupling [11, 12], L-shaped slot [13], differential feed [14], and H-shaped slot [15]—often require complex multilayer networks or multiple ports, resulting in higher losses and larger sizes. However, most dual-linear polarization arrays face challenges achieving high CPLs, wide impedance bandwidths, and compact configurations. Authors in [16] proposed a narrow bandwidth, a poor cross-polarization of -25 dB, and an unfavorable radiation pattern. The proposed design, a single-port, compact, rhombic-feed, co-aligned 2x4 subarray, aims to improve the CPL to -45 dB, achieve a stable reflection coefficient, increase the bandwidth, and exhibit desirable radiation performance.

II. MATERIALS AND METHODS

According to [17], a bandwidth of approximately 300 MHz is sufficient for receiver operation. The Rogers RT/Duroid 5880 substrate was selected for Ku-band applications because of its low dielectric constant (ε_r = 2.2), 1.57-mm thickness, and dielectric loss tangent (tanδ) of 0.0009. These properties contribute to improved radiation efficiency, reduced losses, and a wider bandwidth [18]. The stack-up includes 0.035 mm-thick copper layers for the ground and patch. The antenna was designed and simulated using CST Microwave Studio and its specifications are shown in Table I. Open boundary conditions were applied on all sides to emulate free-space radiation. The antenna was powered using a 50 Ω waveguide port between the feed line and the ground plane; a discrete port was utilized for the dipole antenna configuration. Approximately 2 million mesh cells were used for the main antenna parameter optimization, and up to 100 million cells were used for S21 analysis to ensure convergence accuracy. Figure 1 shows that the proposed CST design uses a rhombic feed on a circular patch to achieve dual linear polarization. Its symmetric, four-branch structure excites two orthogonal TM11 modes with equal path lengths. A single input divides the power symmetrically to produce balanced, high-isolation, high-purity orthogonal polarizations without the need for bulky hybrids or multiple ports.

TABLE I. ANTENNA PARAMETER TARGET

Antenna design parameters	Target
S11	< -14 dB
Bandwidth	> 360 MHz
Gain	> 7 dBi
Polarization	Dual-linearly polarized
Width of the sub-array antenna	Maximum 50 mm

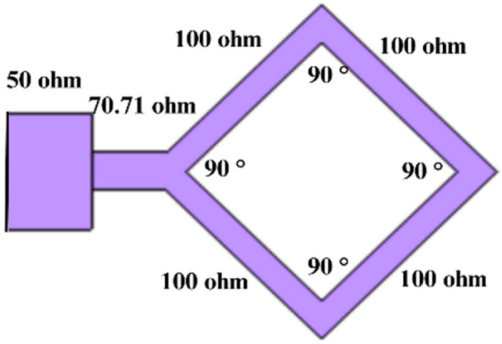

Fig. 1. Feeding design.

The proposed configuration is a compact, single-plane design that is 50 mm wide, allowing for easier integration into phased array systems. The single-port rhombic feed eliminates the need for vias and hybrids, reducing losses and complexity while enabling dual linear polarization. A quarter-wave transformer is used for impedance matching. The characteristic impedance of the transformer, Z_1, is:

$$Z_1 = \sqrt{Z_0 R_{in}} \quad (1)$$

$$l = \frac{\lambda_g}{4} \quad (2)$$

where l is the length of a quarter wavelength with guided wavelength in the medium (λ_g), Z_0 is the input transmission line's characteristic impedance, and R_{in} is the antenna input resistance at resonance. The transformer matches the 100 Ω at the patch input to the 50 Ω at the feed. The intermediate impedance is 70.71 Ω, calculated using the standard equation [19]. Modern communication systems, such as phased array antennas and satellite communications, commonly employ dual linear polarization to enhance data transmission efficiency and minimize inter-channel interference, enabling the transmission of two independent signals at the same frequency with different polarization orientations. Polarization refers to the orientation of an electromagnetic wave's electric field vector ($\vec{E}$) affecting transmission and reception efficiency. Figure 2 shows the two types of linear polarization of the proposed antenna. In the horizontal orientation, E1 oscillates along the x-axis, and E1y = 0. In the vertical orientation, E2 oscillates along the y-axis with E2x = 0, and both propagate along the z-axis. Advanced phased array antennas often use dual linear polarization. The horizontal and vertical modes are enabled simultaneously to increase capacity and robustness. This requires symmetrical

feeds and impedance matching to enable independent operation through either orthogonal feeds or a 90° phase shift.

$$E_1 = E_{1x}\hat{\imath} + E_{1y}\hat{\jmath} = E_{1x}\hat{\imath} \quad (3)$$

$$E_2 = E_{2x}\hat{\imath} + E_{2y}\hat{\jmath} = E_{2y}\hat{\jmath} \quad (4)$$

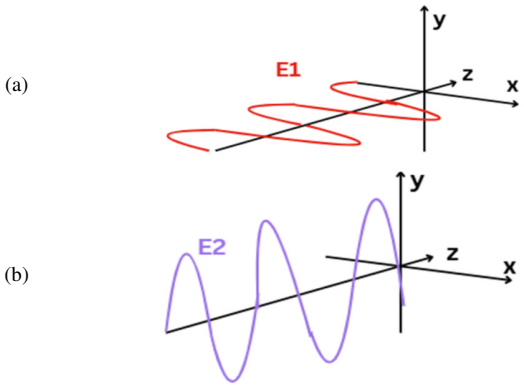

Fig. 2. Dual linear polarization: (a) horizontal polarization, (b) vertical polarization.

III. RESULTS AND DISCUSSION

A. Design of Subarray Antenna

Antenna performance is measured in an anechoic chamber, a room designed to provide a reflection-free environment. Figure 3 (a) depicts the sub-array antenna serving as the receiver mounted on a rotating positioner at the center of the chamber. A spectrum analyzer located outside the chamber was connected to the Antenna Under Test (AUT) along with a reference Vivaldi antenna via an RF switch and power divider, and the received continuous-wave signal was monitored. The AUT was rotated to record radiation patterns. The polarization validation of the subarray antenna was measured, with the transmitter and receiver antennas 1.5 m apart, outside the far-field region [20], as illustrated in Figure 3 (b):

$$R \geq \frac{2D^2}{\lambda} \quad (5)$$

where D is the antenna's largest dimension, and λ is the wavelength of the operating frequency, defining the minimum distance (R) at which an antenna's radiation pattern becomes stable and independent of near-field effects. The measurement used a Ku-band horn reference antenna facing the AUT. Both antennas were connected to the VNA to measure S21 at different polarization alignments: vertical, horizontal, and 45° slant. CPL is:

$$CPL\ (dB) = 20log_{10}\left(\frac{|E_{co-pol}|}{|E_{cross-pol}|}\right) \quad (6)$$

where $E_{co\text{-}pol}$ is the co-polarized and $E_{cross\text{-}pol}$ the cross-polarized field components. The S21 parameter is measured for each orientation, determining whether the maximum received power is greater when the antenna is co-polarized than when it is slanted at a 45° angle. Vertical or horizontal orientation is considered co-polarized. However, when the horn is oriented at a 45° angle, the polarization is considered cross-polarized. The results of this measurement confirm that the subarray antenna supports independent vertical and horizontal polarization. The weaker response at a 45° tilt, due to cross-polarization, further validates its dual-polarization capability.

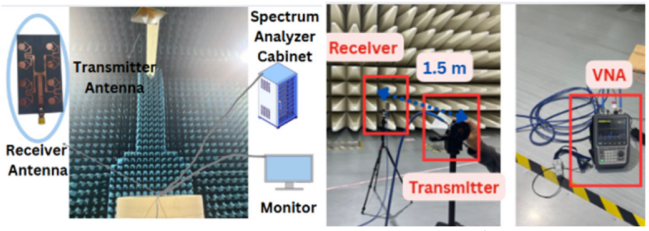

Fig. 3. Measurement scenario: (a) for S11 and Radiation Pattern, (b) for polarization.

B. Simulation and Measurement Results

Authors in [21, 22] examined the compact sub-array technique for dual-polarized antennas, which has a complex design and poses challenges in maintaining a good radiation pattern. The proximity of the radiating elements in a compact subarray can distort the radiation pattern's symmetry, increase mutual coupling, and degrade cross-polarization performance. This study proposes a novel design solution for a compact dual-polarization antenna that addresses these issues. The design integrates a rhombic feed with a co-oriented 2×4 sub-array configuration, ensuring consistent radiation characteristics and enhancing polarization diversity while reducing cross-polarization, as portrayed in Figure 4 and Table II.

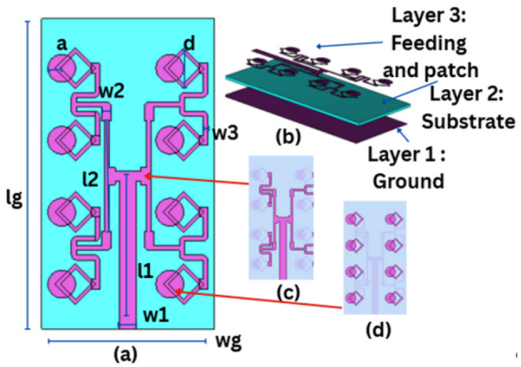

Fig. 4. Subarray antenna design: (a) front view, (b) perspective view, (c) feeding configuration, (d) radiating element configuration.

TABLE II. ANTENNA SUBARRAY DIMENSION

Parameter	Value (mm)
Width of substrate/ground plane (W_g)	50
Length of substrate/ground plane (L_g)	89.6
Radius of the patch (a)	4.01
Length of rhombic-shaped feed (b)	11.8
Width of 50 Ω feed (w_1)	4.878
Width of 70.71 Ω feed (w_2)	2.798
Width of 100 Ω feed (w_3)	1.409
Length of 50 Ω feed (l_1)	42.70
Length of 100 Ω feed (l_2)	32.13

The proposed antenna has three layers: a ground plane, a substrate, and a patch layer. Eight circular patches arranged in a 2×4 subarray are aligned to maintain polarization symmetry and minimize cross-polarization. The transmission line network uses three-quarter square microstrip lines to align power and phase, combined with rhombic feed lines of equal length to ensure balanced amplitude and phase distribution. The rhombic feeds provide symmetrical paths to the input ports of each patch, ensuring balanced excitation in both horizontal and vertical directions. This allows the antenna to generate two independent linear polarizations with high isolation and low cross-polarization. The co-aligned elements in the subarray design ensure a uniform radiation pattern and polarization across the subarray. This alignment minimizes phase errors, reduces mutual coupling, improves beam symmetry, and lowers sidelobe levels. The combination of co-alignment and rhombic feedlines creates balanced excitation, excellent isolation, high polarization purity, and minimal cross-polarization. This supports precise beam control and stable dual polarization performance. The main antenna dimensions include the ground length (l_g), ground width (w_g), and patch size (a). Additionally, the feeder network dimensions (l_1, l_2, w_1, w_2, w_3) are adjusted to ensure impedance matching, current balance, and efficient power transfer. This design improves cross-polarization performance while maintaining bandwidth and radiation quality in a compact, single-port, dual-polarized system. An SMA female jack RF coaxial connector (50 Ω) was used to feed the prototype for measurements. The Vector Network Analyzer (VNA) was calibrated using the standard Short-Open-Load-Thru (SOLT) method prior to measurement. The distance between the AUT and the standard horn antenna in the anechoic chamber was 1.5 m, satisfying the far-field condition (the calculated far-field distance was approximately 0.6 m at 12.5 GHz). According to Figure 5 and Table III, the S11 simulation results are -47.43 dB at 12.55 GHz with a 659 MHz bandwidth. The measurement results show a slight frequency shift from 12.55 GHz to 12.32 GHz, with the S11 value being -20.51 dB and the bandwidth at 364 MHz. However, both the simulation and measurement results meet the required standards, with an S11 value below the -14 dB threshold. This frequency shift is caused by fabrication tolerances and variations in substrate permittivity; small changes in the dimensions or spacing of elements can slightly alter the resonance frequency. In Figure 6, the antenna radiation pattern is displayed and evaluated over a range of 0° to 360°. The simulation and measurement results reveal a directional radiation pattern that effectively directs energy toward the intended target. This characteristic is ideal for applications requiring concentrated radiation, such as satellite communication systems. The main lobe achieves peak gain values of 9.28 dBi and 8.77 dBi in the simulation and measurement, respectively. Figure 7 (a) demonstrates that the S21 simulation results for vertical and horizontal orientations are -48.68 dB and -50.75 dB, respectively, which are greater than the -67.71 dB value at a 45-degree slant. Figure 7 (b) shows that the measurement results exhibit the same trend, with S21 values of -45.41 dB and -45.63 dB for vertical and horizontal polarizations, respectively. When the transmitter is oriented at a 45-degree slant, the value drops to -48.48 dB. These results confirm that the co-polarized S21 is much higher than the cross-polarized S21, indicating good polarization purity.

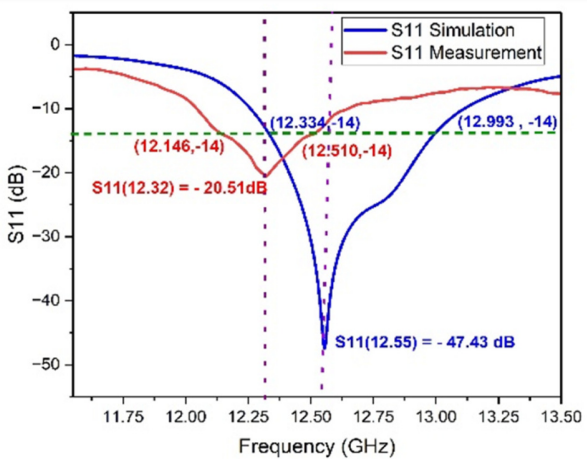

Fig. 5. S_{11} comparison.

TABLE III. ANTENNA PARAMETER RESULTS

Parameters	Simulation	Measurement
S11	-47.43 dBi	-20.51 dBi
Bandwidth	659 MHz	364 MHz
Gain	9.25 dBi	8.77 dBi
Polarization	Dual-linearly polarized	Dual-linearly polarized
CPL	< - 45 dB	< -45 dB
Dimension	50×89.6×1.64 mm	50.04 × 89.57 × 1.64 mm

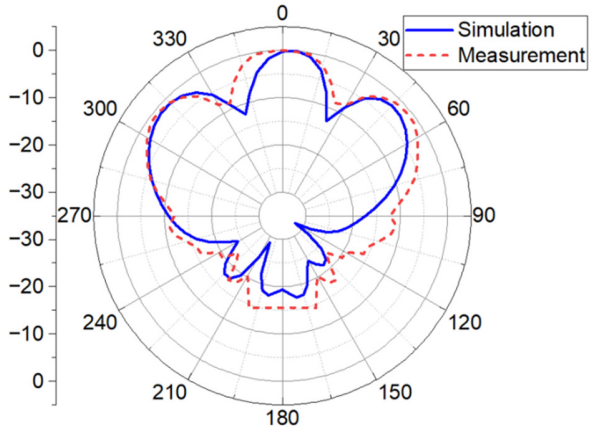

Fig. 6. Radiation pattern.

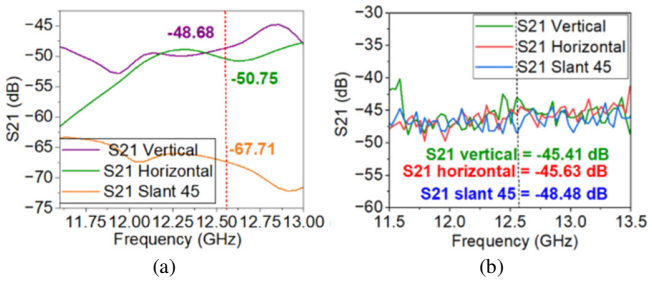

(a) (b)

Fig. 7. (a) S21 simulation, and (b) S21 measurement.

As depicted in Figure 8 (a), the co-polarization level is -48.68 dB in the vertical orientation and -50.75 dB in the horizontal orientation. However, the CPL at a 45° slant reaches -67.71 dB. These results indicate high polarization discrimination and minimal unwanted cross-polarized radiation components. The CPL results achieved in this study are approximately twice as good as those reported in [16], where the values only ranged from -25 to -30 dB. This demonstrates the effectiveness of antenna design optimization in suppressing CPLs. The measurement results presented in Figure 8 (b) show co-polarization levels of -45.41 and -45.63 dB in the vertical and horizontal orientations, respectively, while the CPL at a 45° slant decreases to -48.48 dB. Cross-polarization cancellation in the proposed antenna is achieved through the geometric symmetry of its elements and a carefully designed rhombic differential feed. This feed provides balanced amplitude and phase to cancel unwanted orthogonal fields. Co-oriented elements in optimization space enhance constructive interference on co-polarized fields. Destructive interference on cross-polarized components effectively suppresses cross-polarization, ensuring high polarization purity.

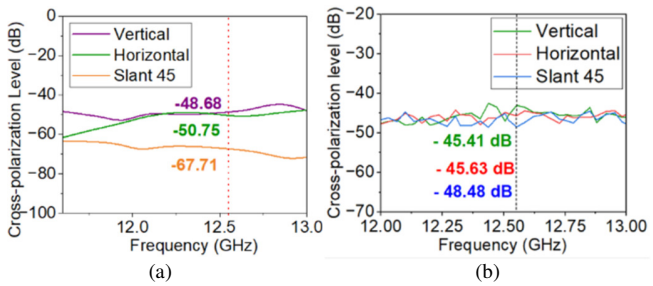

(a) (b)

Fig. 8. CPL: (a) simulation, (b) measurement.

In Table IV, the designed antenna is compared with other antennas [23–26] based on several parameters, including size, bandwidth, gain, and CPL. Unlike most systems, which use multiple ports, the proposed design has the advantage of a single-port configuration, which simplifies the feed structure and reduces complexity. While other designs achieve higher gains of 17.26, 14.35, 24.5, and 22.7 dBi, they require larger dimensions and more complex geometry.

TABLE IV. COMPARISON OF PROPOSED WORK WITH LITERATURE WORK

Ref.	Dimension (mm)	Bandwidth (MHz)	Gain (dbi)	CPL (dB)
[12]	4×10 elements (119.4×298.5×7.35)	200	17.26	<-45
[13]	1×8 elements (34.2×273.6× 0.16)	50	14.35	<-40
[14]	1 element (5.5 × 5.5 ×1.69)	4000	5.74	<-30
[16]	2×4 elements (50 × 96.5 × 1.64)	360	8.99	<-25
[23]	8×8 elements (131.1×131.1× 3.8)	19000	24.5	<-45
[24]	8×8 elements (94 × 94 × 2.77)	750	22.7	<-25
[25]	5×5 elements (24 × 24× 2)	800	17	<-30
[26]	1 element (25× 25 × 3.5)	180	5.8	<-40
This work	2×4 elements (50×89.6×1.64)	659	9.25	<-45

Authors in [24, 25] revealed a wider bandwidth, with degraded CPL of less than -30 dB or -25 dB. Authors in [23, 26] relied on a dual or large port structure. Traditional microstrip designs often have a narrow bandwidth [27]. Despite using a single port, the proposed antenna increases the bandwidth from 360 MHz to 659 MHz, the gain increases from 8.99 dBi to 9.25 dBi, and the CPL decreases from -25 dB to -45 dB, confirming a balanced trade-off between size, performance, and polarization purity. The design is, thus, suitable for practical Ku-band satellite receivers. The proposed design offers several advantages: dual linear polarization; a significantly improved cross-polarization level; a compact, single-port architecture with a rhombic feed; and enhanced bandwidth and gain compared to the previous designs.

IV. CONCLUSIONS

The proposed 2×4 compact microstrip circular patch subarray, with co-aligned elements and a rhombic feed, has an overall size of 50×89.6×1.64 mm. The subarray achieves dual linear polarization, as verified by S21, with a Cross-Polarization Level (CPL) below –45 dB—an improvement over the –25 dB, as reported in [16]. The simulation and measurement results meet the target parameters. The subarray antenna has a simulated gain of 9.28 dBi and a measured gain of 8.77 dBi. Its bandwidths are 659 MHz and 364 MHz, respectively, showing an 83% improvement in simulated bandwidth, exceeding the 360 MHz threshold. Despite a frequency shift from 12.55 GHz to 12.32 GHz due to fabrication errors and material tolerances, the antenna maintains stable performance within the Ku band. These results suggest that the co-aligned array geometry and the optimized rhombic feeding structure effectively enhance the gain and bandwidth while suppressing the cross-polarization. This makes the design suitable for compact Ku-band mobile communication satellite receivers.

ACKNOWLEDGMENT

Universitas Indonesia funded this research through the International Indexed Publication (PUTI) Hi-Impact Grant, 2025, number: PKS-41/UN2.RST/ HKP.05.00/2025. The Indonesian Digital Test House (IDTH), under the Ministry of Communication and Information of the Republic of Indonesia, has provided measurement facilities to support this research.

REFERENCES

[1] A. N. Nikicio, J. D. Setiawan, W. Hasbi, and D. Wood, "The Potential Role of Satellite IoT in Disaster Risk Reduction in Indonesia," in *72nd International Astronautical Congress*, Dubai, UAE, Oct. 2021.

[2] B. Maruddani, E. Sandi, and W. Dara, "Study of Nusantara Satu Satellite parameter evaluation for broadband application in Indonesia," *Journal of Physics: Conference Series*, vol. 1402, no. 4, Sept. 2019, Art. no. 044027, https://doi.org/10.1088/1742-6596/1402/4/044027.

[3] J. Kim, "A Review of Ku-Band GaN HEMT Power Amplifiers Development," *Micromachines*, vol. 15, no. 11, Nov. 2024, Art. no. 1381, https://doi.org/10.3390/mi15111381.

[4] F. Al-Janabi, M. J. Singh, and A. P. S. Pharwaha, "Development of Microstrip Antenna for Satellite Application at Ku/Ka Band," *Journal of Communications*, vol. 14, no. 6, pp. 118–125, 2021, https://doi.org/10.12720/jcm.16.4.118-125.

[5] Y. S. Gurbet and S. Doğu, "Comprehensive Review of Ku, K, and Ka Band Antenna Designs: Applications in CubeSats," *International Journal of Aeronautical and Space Sciences*, June 2025, https://doi.org/10.1007/s42405-025-00989-5.

[6] M.-A. Chung, K.-C. Tseng, and I.-P. Meiy, "Antennas in the Internet of Vehicles: Application for X Band and Ku Band in Low-Earth-Orbiting

Satellites," *Vehicles*, vol. 5, no. 1, pp. 55–74, Mar. 2023, https://doi.org/10.3390/vehicles5010004.

[7] P. Sanchez-Olivares, J.-L. Masa-Campos, E. Garcia-Marin, D. Barrio-Tejedor, and P. Kumar, "Dual-linearly polarized travelling-wave array antenna based on triple plus slots fed by square waveguide," *AEU - International Journal of Electronics and Communications*, vol. 119, May 2020, Art. no. 153176, https://doi.org/10.1016/j.aeue.2020.153176.

[8] Y. Fan, X. Liu, H. Yang, and Z. Ju, "Dual Circularly Polarized Textile Antenna with Dual Bands and On-/Off-Body Communication Modes for Multifunctional Wearable Devices," *Electronics*, vol. 14, no. 9, Jan. 2025, Art. no. 1898, https://doi.org/10.3390/electronics14091898.

[9] Z. Cui *et al.*, "Improving GNSS-R Sea Surface Altimetry Precision Based on the Novel Dual Circularly Polarized Phased Array Antenna Model," *Remote Sensing*, vol. 13, no. 15, Jan. 2021, Art. no. 2974, https://doi.org/10.3390/rs13152974.

[10] T. Alam *et al.*, "Metamaterial Based Ku-Band Antenna for Low Earth Orbit Nanosatellite Payload System," *Nanomaterials*, vol. 13, no. 2, Jan. 2023, Art. no. 228, https://doi.org/10.3390/nano13020228.

[11] W. Zhang, H. Sun, G. Song, T. Zhang, Y. Wang, and Z. Liu, "Ku Band Dual-Polarized Microstrip Array Antenna with Wide-Band and Low Side-Lobe," in *2019 IEEE 2nd International Conference on Electronic Information and Communication Technology (ICEICT)*, Harbin, China, Jan. 2019, pp. 374–377, https://doi.org/10.1109/ICEICT.2019.8846427.

[12] H. Saeidi-Manesh and G. Zhang, "Low Cross-Polarization, High-Isolation Microstrip Patch Antenna Array for Multi-Mission Applications," *IEEE Access*, vol. 7, pp. 5026–5033, 2019, https://doi.org/10.1109/ACCESS.2018.2889599.

[13] J. Zeng, X. Lin, Y. Yang, T. Qin, and Y. Kang, "High-Isolation, Low Cross-Polarization, Differential-Feed, Dual-Polarized Patch Antenna Array for a 2.45 GHz Retrodirective System Application," in *2020 IEEE Asia-Pacific Microwave Conference (APMC)*, Hong Kong, Hong Kong, Sept. 2020, pp. 193–195, https://doi.org/10.1109/APMC47863.2020.9331487.

[14] L. Ma, C. Che, Z. Zhang, and Y. Wang, "Design of a Dual-Polarized Microstrip Antenna with High Cross-Polarization Isolation," in *2023 16th UK-Europe-China Workshop on Millimetre Waves and Terahertz Technologies (UCMMT)*, Guangzhou, China, Dec. 2023, vol. 1, pp. 1–3, https://doi.org/10.1109/UCMMT58116.2023.10310395.

[15] M. Kai, F. Hou, and D. Sun, "Design of a broadband dual-polarized mircostrip antenna array with high isolation," in *2017 Sixth Asia-Pacific Conference on Antennas and Propagation (APCAP)*, Xi'an, China, July 2017, pp. 1–3, https://doi.org/10.1109/APCAP.2017.8420417.

[16] R. J. Yanti, A. I. Wahdiyat, E. T. Rahardjo, F. Y. Zulkifli, and C. Apriono, "Design of a circular patch sub-array microstrip antenna with dual linear polarization for Ku-band satellite communication applications," *e-Prime - Advances in Electrical Engineering, Electronics and Energy*, vol. 11, Mar. 2025, Art. no. 100939, https://doi.org/10.1016/j.prime.2025.100939.

[17] R. Vincenti Gatti, L. Marcaccioli, E. Sbarra, and R. Sorrentino, "Flat array antenna for Ku-band mobile satellite terminals," in *Proceedings of the 5th European Conference on Antennas and Propagation (EUCAP)*, Rome, Italy, Apr. 2011, pp. 2618–2622.

[18] B. S. Deepak, R. N. Kumar, M. Madhavi, P. Avinash, and K. Yaswanth, "Design of A Handy Tripleband Micro- Strip Patch Antenna for Satellite Based IoT Applications," *International Journal of Innovative Technology and Exploring Engineering (IJITEE)*, vol. 8, no. 6, pp. 2278–3075, 2019.

[19] F. I. Obiadi and M. K. Udofia, "Comparative Analysis of Microstrip Antenna Arrays with Diverse Feeding Techniques," *Journal of Engineering Research and Reports*, vol. 26, no. 1, pp. 18–38, Jan. 2024, https://doi.org/10.9734/jerr/2024/v26i11060.

[20] A. Capozzoli, C. Curcio, F. D'Agostino, and A. Liseno, "A Review of the Antenna Field Regions," *Electronics*, vol. 13, no. 11, Jan. 2024, Art. no. 2194, https://doi.org/10.3390/electronics13112194.

[21] R. J. Yanti, C. Apriono, E. T. Rahardjo, and F. Yuli Zulkifli, "Dual Linearly Polarized 2x4 Subarray Antenna for Phased Array System in Satellite Communications," in *2024 IEEE Asia-Pacific Conference on Applied Electromagnetics (APACE)*, Langkawi, Kedah, Malaysia, Sept. 2024, pp. 112–115, https://doi.org/10.1109/APACE62360.2024.10877302.

[22] R. J. Yanti, C. Apriono, E. T. Rahardjo, and F. Y. Zulkifli, "Design of A Compact Linearly Dual Polarized Series-Fed Phased Array Antenna Using Rhombus Feeding Technique for Ku-Band Satellite Communications," in *2024 IEEE Asia-Pacific Microwave Conference (APMC)*, Bali, Indonesia, Aug. 2024, pp. 366–368, https://doi.org/10.1109/APMC60911.2024.10867466.

[23] Y. J. Cheng, F. Y. Tan, M. M. Zhou, and Y. Fan, "Dual-Polarized Wideband Plate Array Antenna With High Polarization Isolation and Low Cross Polarization for D-Band High-Capacity Wireless Application," *IEEE Antennas and Wireless Propagation Letters*, vol. 19, no. 12, pp. 2023–2027, Sept. 2020, https://doi.org/10.1109/LAWP.2020.3020385.

[24] H. Li, Y. Ma, F. Cui, G. Yin, H. Wu, and Y. Ren, "Broadband dual polarization microstrip array suitable for Ku -band satellite communication," in *2024 IEEE 12th Asia-Pacific Conference on Antennas and Propagation (APCAP)*, Nanjing, China, Sept. 2024, pp. 1–2, https://doi.org/10.1109/APCAP62011.2024.10881975.

[25] X. Liu, Z. Qu, Y. Yao, and Y. Gao, "X/Ku-Band Shared-Aperture Phased Array With Low-Frequency Ratio and High Isolation," *IEEE Transactions on Antennas and Propagation*, vol. 73, no. 10, pp. 7388–7398, July 2025, https://doi.org/10.1109/TAP.2025.3583135.

[26] W. Huang, X.-X. Yang, and J. Du, "A Miniaturized Dual-Polarized Antenna With High Isolation and Low Cross Polarization," *IEEE Antennas and Wireless Propagation Letters*, vol. 24, no. 5, pp. 1075–1079, Feb. 2025, https://doi.org/10.1109/LAWP.2025.3525719.

[27] M. Nahas, "A Multi-Slotted Multi-Band Microstrip Patch Antenna Design for 5G Communication Devices," *Engineering, Technology & Applied Science Research*, vol. 15, no. 4, pp. 24605–24610, Aug. 2025, https://doi.org/10.48084/etasr.11441.